Applied Physics B (2018) 124:179
https://doi.org/10.1007/s00340-018-7053-3

Applied Physics B
Lasers and Optics

Efficient Ho:YAP laser dual end-pumped by a laser diode at 1.91 μm in a wing-pumping scheme

Xiaoming Duan[1] · Linjun Li[2] · Yingjie Shen[3] · Baoquan Yao[1]

Received: 4 June 2018 / Accepted: 16 August 2018 / Published online: 20 August 2018

Abstract
We demonstrated a first continuous-wave and acousto-optical Q-switched Ho:YAP laser pumped by fiber-coupled laser diode at 1.91 μm. With a dual-end wing-pumping scheme, a maximum continuous-wave output power of 10.5 W at 2.1 μm and a slope efficiency of 53.2% were obtained when the incident LD power was 25.6 W, while diode-to-Ho conversion efficiency reached up to 41.0%. The Q-switched Ho:YAP laser was investigated for different pulse repetition frequencies from 3 to 20 kHz. The maximum average output power of 9.8 W and maximum pulse energy of 2.7 mJ were achieved at pulse repetition frequencies of 20 and 3 kHz, respectively. In addition, we demonstrated an efficient mid-infrared laser based on a diode-Ho-ZGP architecture for the first time. With a pulse repetition frequency of 3 kHz and an incident Ho pump power of 8.2 W, the average output power of 4.8 W and slope efficiency of 61.0% were reached in mid-infrared ZGP-OPO.

1 Introduction

High-power 2-μm laser sources are very important in many scientific and technical applications such as medical, wind lidar, remote sensing, and mid-infrared nonlinear optical conversion [1–3]. The laser diode (LD) pumped thulium (Tm) laser is the first scheme to realize the all solid-state 2 μm lasers. Two advantages of this laser, namely high-efficiency pumping (commercial LD around 800 nm), and high quantum efficiency (two-for-one cross-relaxation process), enable the Tm laser to yield hundreds of watts of output power in the 1.9–2 μm spectral region [4, 5]. However, for some applications, Tm lasers are not suitable due to its short operating wavelength.

In contrast, holmium (Ho) lasers based on the $^5I_7 \rightarrow {}^5I_8$ transition produces wavelengths longer than 2.05 μm. Meanwhile, the Ho ion has a larger emission cross section and longer upper state lifetime for the 2 μm laser transition, so it is more suitable to achieve high-power and high-energy 2 μm laser radiations. For an efficient 2-μm Ho laser, a 1.9-μm resonant pumping scheme is required for room-temperature operation. The main advantage is the low quantum defect, which creates the excellent characteristics of low thermal load, high efficiency, and high power of 2-μm Ho lasers. In the past two decades, resonantly pumped Ho lasers have been widely investigated. There are two methods to realize resonant pumping of Ho lasers. First, a Tm laser is used as the pump source due to its high power, narrow linewidth, and high beam quality in the 1.9-μm spectral region. Nowadays, up to 81.2% slope efficiency [6] or 103 W output power [7] was reported from this approach. Unfortunately, this cascading scheme increases the packaging size and decreases the diode-to-Ho conversion efficiency of the whole system. A feasible solution to overcome these issues is to use 1.9-μm laser diodes as an alternative to Tm lasers. As early as 1995, Nabors et al. reported the first 1.9 μm LD-pumped Ho:YAG laser with output power of 0.67 W and slope efficiency of 35% at an operating temperature of 220 K [8]. In 2008, Scholle et al. employed LD stacks as the pump source to obtain a 40-W continuous-wave (CW) Ho:YAG laser with slope efficiency of 57% with respect to the absorbed pump power [9]. Later, by using the same LD pump source, Lamrini et al. optimized the output performances of the Ho:YAG laser [10, 11] and demonstrated a novel Ho:Lu_2O_3 laser [12]. At present, commercial high-power fiber-coupled LDs operating at 1.9 μm are available for a compact

✉ Xiaoming Duan
xmduan@hit.edu.cn

1 National Key Laboratory of Tunable Laser Technology, Harbin Institute of Technology, Harbin 150001, China

2 Heilongjiang Province Key Laboratory of Optoelectronics and Laser Technology, Heilongjiang Institute of Technology, Harbin 150050, China

3 School of Opto-Electronic Information Science and Technology, Yantai University, Yantai 264005, China

structure. In 2011, Jambunathan et al. reported a new CW $Ho:KLu(WO_4)_2$ laser with output power of 408 mW and slope efficiency of 54.5% with respect to the absorbed pump power [13]. In 2011, Newburgh et al. demonstrated that fiber-coupled LD-pumped crystalline $Ho:YVO_4$ and ceramic $Ho:Y_2O_3$ laser produced output power of 1.6 and 2.5 W at the operating temperature of 77 K [14, 15], respectively. In 2015, with two fiber-coupled LDs providing 53 W pump power and a 5/65/5-mm-long composite crystal, Berrou et al. reported a CW and Q-switched Ho:YAG laser at 2121 nm with CW output power of 18 W and slope efficiency of 51% with respect to the absorbed pump power [16]. In 2017, Ji et al. reported slope efficiency of 89.2% with respect to absorbed pump power from a Ho:YLF laser pumped by a fiber-coupled LD [17]. However, the diode-to-Ho conversion efficiency of these lasers is unsatisfactory because of the low pump spectral brightness, bad pump mode overlap, or weak pump absorption. For example, only about 25% diode-to-Ho conversion efficiency was achieved in Ref. [17].

For most 1.9-μm LDs, the central wavelength fluctuates with its operating temperature, which leads to unstable pump absorption efficiency in the Ho crystal due to the narrow absorption characteristics of the Ho crystal. In particular, there is obvious difference at the same pump absorption peaks along different polarized directions in most anisotropy Ho crystals. This difference leads to unacceptable output power fluctuations under random unpolarized pumping conditions [18]. Therefore, strong and stable pump absorption is necessary to achieve high diode-to-Ho conversion efficiency.

Among Ho-doped materials, $Ho:YAlO_3$ (Ho:YAP) crystal is an attractive gain medium for 2-μm laser [19]. The absorption data of Ho:YAP crystal were achieved in our previous work [20] (see Fig. 1), and it has almost equivalent absorption cross sections of 0.4×10^{-20} cm^2 around 1910 nm for the three crystallographic axes. Additionally, the absorption curve is near flat around this wavelength, and it is far away from the absorption peaks of Ho:YAP, which is called wing-pumping scheme [21]. This is very beneficial to stabilize the pump absorption efficiency of the Ho:YAP crystal. Up to present, by using Tm-bulk or Tm-fiber lasers as the pumping source, many CW, Q-switched [22–25] or mode-locked [26] Ho:YAP lasers were reported. The maximum output power of 31.4 W and minimum pulse width of 254.8 ps were achieved in Refs. [25, 26], respectively. However, as we know, there is no report on the LD directly pumped Ho:YAP laser.

In this paper, we demonstrated, for the first time to our knowledge, a room-temperature CW and acousto-optical Q-switched Ho:YAP laser dual end-pumped by a fiber-coupled LD at 1.91 μm in a wing-pumping scheme. At the operating temperature of 15 °C, the CW Ho:YAP laser produced a maximum output power of 10.5 W and a slope efficiency of 53.2% when the incident pump power was 25.6 W. Up to 41.0% diode-to-Ho conversion efficiency was achieved. The beam quality factor (M^2) was estimated to be 1.4 at the maximum output level. At the pulsed repetition frequencies (PRFs) of 3 kHz, 5 kHz, 10 kHz, 15 kHz and 20 kHz, we investigated the output performances of the Q-switched Ho:YAP laser. At PRF of 20 kHz, the Q-switched Ho:YAP laser produced average output power of 9.8 W and slope efficiency of 49.4% with respect to the incident LD power. In addition, we demonstrated an efficient mid-infrared laser based on the diode-Ho-ZGP architecture. At a PRF of 3 kHz and Ho pump power of 8.2 W, the ZGP-OPO yielded average output power of 4.8 W and slope efficiency of 61.0%. The overall optical conversion efficiency from LD to middle infrared was up to 18.8%.

2 Experimental setup

Figure 2 shows a schematic diagram of the experimental setup of Ho:YAP laser for CW and Q-switched operation. In order to reduce the thermal effect of the Ho:YAP crystal,

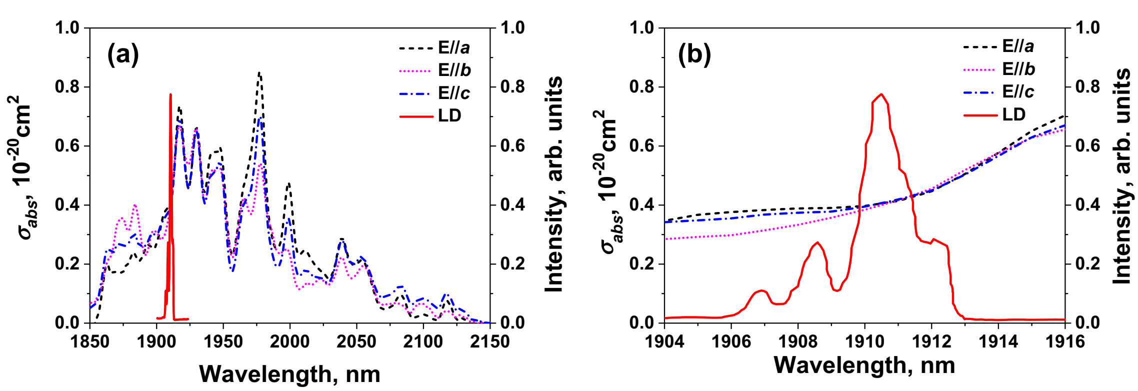

Fig. 1 The absorption spectrum of Ho:YAP crystal and the emission spectrum of the LD under **a** wavelength range of 1860–2160 nm, **b** wavelength range of 1904–1916 nm

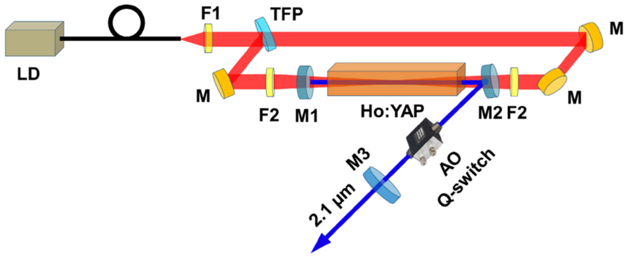

Fig. 2 Experimental setup of Ho:YAP laser dual end-pumped by LD

a dual end-pumping structure was used in this experiment. Furthermore, in order to avoid the LD being affected by the undepleted 1.9-µm pump light, a thin film polarizer (TFP) was used as the beam splitter, which has high transmission for *p*-polarized pump light and high reflectivity for *s*-polarized pump light. A 40-W fiber-coupled LD at approximately 1.91 µm was used as the pump source with a pigtail fiber core diameter of 600 µm and numerical aperture of 0.22. The emission spectrum of LD was recorded by an optical spectrum analyzer (Bristol 721A), as shown in Fig. 1. The central emission wavelength of LD was set to keep away from the absorption peaks of Ho:YAP crystal. It was centered at about 1910.5 nm with a full width at half-maximum (FWHM) linewidth of less than 2 nm at LD power of 30 W. The central wavelength shift of about 5 nm was recorded from LD threshold to 30 W output power. The unpolarized LD pump light was collimated by a CaF_2 lens F1 with a focal length of 30 mm and then separated by a TFP into two orthogonally polarized beams. Three flat mirrors M had high reflectivity for the pump light and were used to fold the pump beam appropriately. The *p*-polarized pump light was focused into the Ho:YAP crystal with a lens F2 (30 mm focal length), and the *s*-polarized pump light was focused into the crystal by another same lens identical to F2 into the other end of the Ho:YAP crystal. The LD pump diameter was approximately 600 µm. We measured the pump powers before TFP and after M1 and M2, and calculated pump transmission to be about 90%.

The *b*-cut Ho:YAP crystal was used in our studies had dimensions of 2.5 mm × 2.5 mm (in cross section) × 20 mm (in length) and Ho ions concentration of 1.5 at.%. Under no-lasing conditions, the single-pass pump absorption of Ho:YAP crystal was measured to be approximately 78% under LD powers of 5 W and 15 W, which was caused by almost constant absorption cross section of Ho:YAP crystal from 1905 nm to 1910 nm. Both end faces of the crystal were anti-reflection (AR) coated at both pump and laser wavelengths. The crystal was mounted in a copper heatsink with a 0.1-mm-thick indium foil. The temperature of the heatsink was controlled at 15 °C by a thermoelectric cooler. We used an L-shaped cavity with physical length of 70 mm

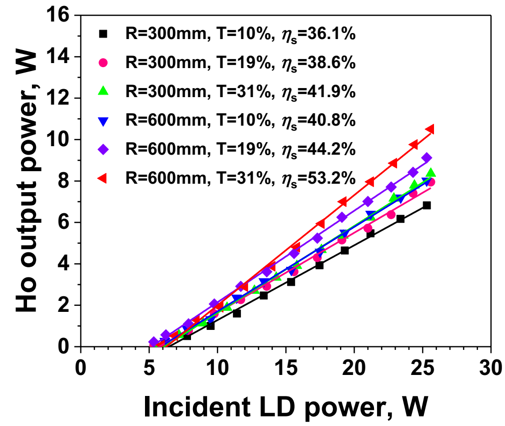

Fig. 3 CW output characteristics of diode-pumped Ho:YAP laser

to realize the dual end-pumping. The 0° dichroic mirror M1 had high transmission (T = 99.5%) at 1.91 µm and high reflectivity (R = 99.7%) at 2.1 µm. The curvature-free 45° dichroic mirror M2 had high transmission (T = 99.7%) at the 1.91 µm and high reflectivity (R = 99.8%) at 2.1 µm. A plano-concave mirror was used as the output coupler M3. A quartz acousto-optic Q-switch with length of 35 mm and aperture of 2.0 mm was employed for Q-switching operation. It had more than 55% diffraction efficiency. Its rated radio frequency power is 20 W at a frequency of 41 MHz. The output couplers with two curvatures (R = 300 mm and 600 mm) were used in this experiment. With ABCD matrix method, we estimated that the Ho laser beam diameters on the acousto-optic Q-switch were approximately 0.56 and 0.64 mm for R = 300 mm and 600 mm, respectively.

3 Experimental results and discussion

A Coherent PM30 power meter was used to measure the output powers of all of the laser configurations in this work. By using three transmittances (T = 10%, 19% and 31%), we investigated the CW output characteristics of the Ho:YAP laser. Figure 3 shows that the output coupler with a curvature of 600 mm and transmission of 31% yields the best power characteristics. The laser threshold was 5.9 W incident LD power. Compared with previous work [20], the pump threshold is higher, which is mainly caused by the bad beam quality (M^2 ~ 109) of the LD pump beam. The Ho:YAP laser reaches CW output power of 10.5 W and slope efficiency of 53.2% under total incident LD pump power of 25.6 W, corresponding to diode-to-Ho conversion efficiency of 41.0%. To the best of our knowledge, this is the highest diode-to-Ho conversion efficiency in 2-µm Ho lasers. In the case of T = 31%, we estimated the beam quality of Ho:YAP laser with two output coupler curvatures (R = 300 mm,

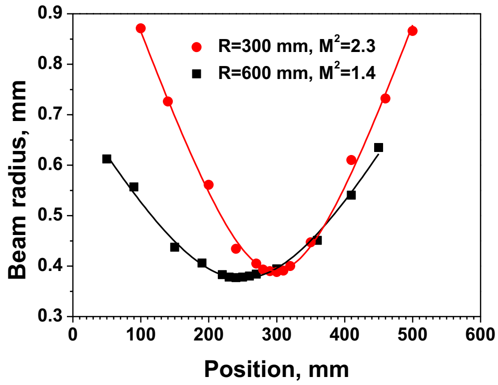

Fig. 4 M^2 measurement of CW Ho:YAP laser

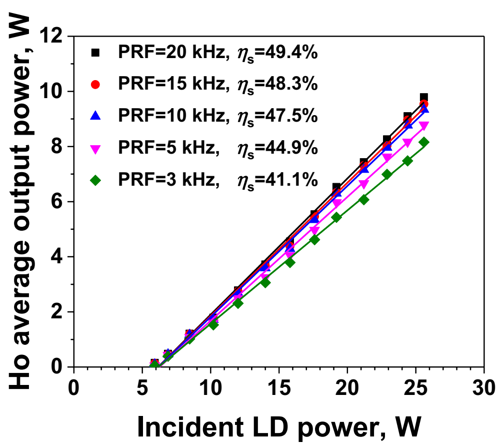

Fig. 5 The Q-switched output performances of Ho:YAP laser

$R=600$ mm) at the maximum output level, as shown in Fig. 4. With the 90/10 knife-edge method, the beam quality factors were calculated to be 2.3 and 1.4 for $R=300$ mm and 600 mm, respectively. This difference was mainly caused by mode overlap of the pump and laser in the cavity. With ABCD matrix method, laser beam diameters in the Ho:YAP crystal were calculated to be 0.49 and 0.59 mm for $R=300$ and 600 mm, respectively. As a result, for 600 μm pump diameter, the better mode overlap of the LD and the Ho-cavity was obtained with $R=600$ mm.

By using the output coupler with a curvature of 600 mm and transmittance of 31%, we investigated the Q-switched performances of the diode-pumped Ho:YAP laser. Figure 5 shows the average output powers of the Q-switched Ho:YAP laser under the PRFs of 3 kHz, 5 kHz, 10 kHz, 15 kHz and 20 kHz. In the case of a PRF of 20 kHz, the Q-switched Ho:YAP laser reached average output power of 9.8 W and slope efficiency of 49.4% with respect to the incident LD power. The Ho laser pulses were detected by an InGaAs photodiode and recorded by a 300-MHz Tektronix digital oscilloscope (DPO 3032). Figure 6 shows the pulse widths, pulse energies and peak powers under different PRFs. When the incident LD pump power was 25.6 W, the minimum pulse widths were 15 ns, 18 ns, 23 ns, 32 ns and 42 ns for the PRF of 3 kHz, 5 kHz, 10 kHz, 15 kHz and 20 kHz, respectively. The maximum single pulse energies for the PRF of 3 kHz, 5 kHz, 10 kHz, 15 kHz and 20 kHz were approximately 2.7 mJ, 1.8 mJ, 0.9 mJ, 0.6 mJ and 0.5 mJ, respectively, corresponding to the calculated maximum peak powers of about 181.3 kW, 97.7 kW, 40.6 kW, 19.9 kW and 11.7 kW.

An optical spectrum analyzer (Bristol 721A) was used to measure the output spectrum of the Ho:YAP laser under CW and Q-switching mode, as shown in Fig. 7. The central wavelengths were 2118.3 and 2115.2 nm for CW and Q-switching mode, respectively. In the Q-switching regime, the lasing wavelength shows a small blue shift due to the increasing cavity losses.

Among numerous applications of 2-μm lasers, acting as the pump source of middle infrared OPOs is important. By using the above diode-pumped Q-switched Ho:YAP laser as the pump source, we investigated the output performances of mid-infrared ZGP-OPO. To the best of our knowledge, this is first mid-infrared laser source based on a diode-Ho-ZGP architecture. In this experiment, a 20.0-mm-long ZGP crystal (Type I, 55° to the *c*-axis) with cross section of 6 mm × 6 mm was employed as the OPO medium. The ZGP crystal was AR-coated for the pump and middle infrared range. It was packed in indium foil (0.05 mm thickness) and mounted into a copper heatsink. A simple linear cavity was used, which is shown in the insert of Fig. 8. This OPO cavity consists of flat mirrors M4 and M5. M4 had high transmission ($T>99\%$) at 2.1 μm and high reflectivity ($R>99.5\%$) for the 3–5 μm spectral region, and M5 has high transmission ($T>99\%$) at 2.1 μm and transmittance of 50% around 3–5 μm. With a focus lens F3 (100 mm focal length), the Ho pump light was focused to about 750 μm in diameter. The physical length of the OPO cavity was approximately 35 mm. A flat mirror M6 was used as the 45° dichroic mirror with high transmission ($T\sim99\%$) for the mid-infrared region and high reflectivity ($R\sim99.5\%$) at 2.1 μm. The mid-infrared beam is the combined sum of the signal wave and idler wave. Figure 8 shows the average output powers of the ZGP-OPO under different PRFs of 3 kHz, 5 kHz, 10 kHz, 15 kHz and 20 kHz. At a PRF of 3 kHz, the ZGP-OPO yields maximum average output power of 4.8 W and slope efficiency of 61.0% with an incident Ho pump power of 8.2 W. The optical conversion efficiency from LD to middle infrared was 18.8%, which was the highest reported value to our knowledge. In addition, in the case of PRF of 10 kHz, the highest slope efficiency of 64.2% was achieved in this experiment.

Figure 9 shows the output spectrum of the ZGP-OPO, which was measured by a 300-mm monochromator and an HgCdTe detector. The central wavelengths of the signal and idler were 4076 and 4414 nm, respectively,

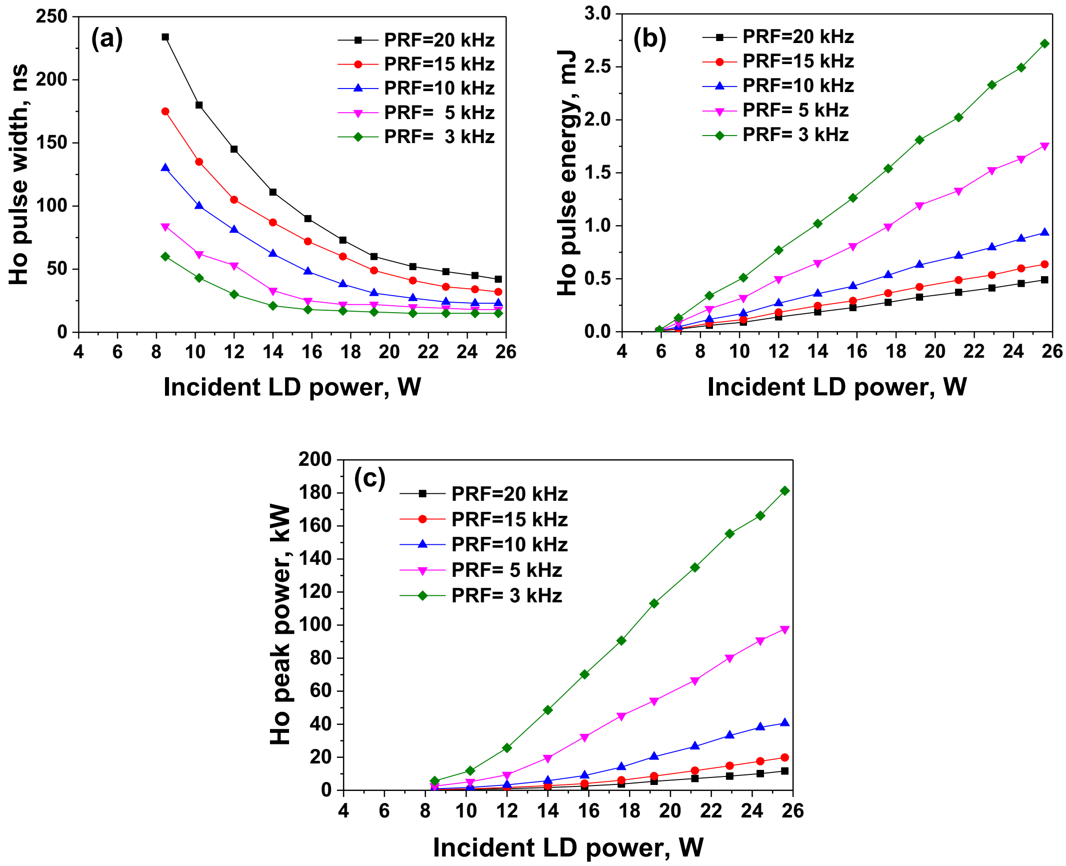

Fig. 6 The dependences of **a** pulse widths, **b** pulse energies and **c** peak powers on PRFs in cases of PRF = 3 kHz, 5 kHz, 10 kHz, 15 kHz and 20 kHz

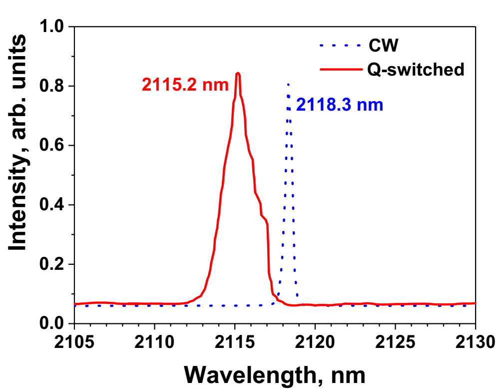

Fig. 7 The output spectrum of Ho:YAP laser with CW and Q-switched mode

corresponding with the FWHM linewidth of about 150 and 130 nm. Finally, with a PRF of 3 kHz, the beam quality factor of ZGP-OPO was measured by the 90/10 knife edge technique at the maximum output level. This M^2 factor was calculated to be 2.8 for the signal and 2.6 for the idler.

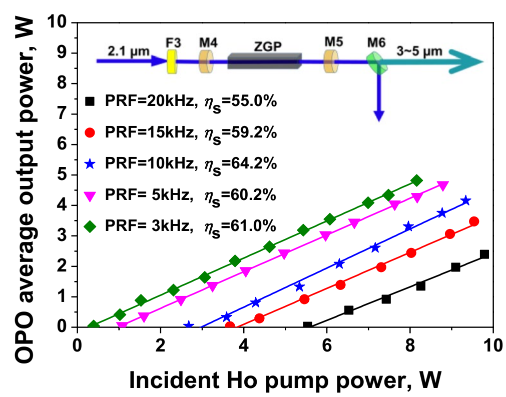

Fig. 8 The total average output power of middle infrared signal and idler wave

4 Conclusion

In summary, we have demonstrated a room-temperature CW and acousto-optical Q-switched Ho:YAP laser dual end-pumped by a fiber-coupled LD at 1.91 μm in

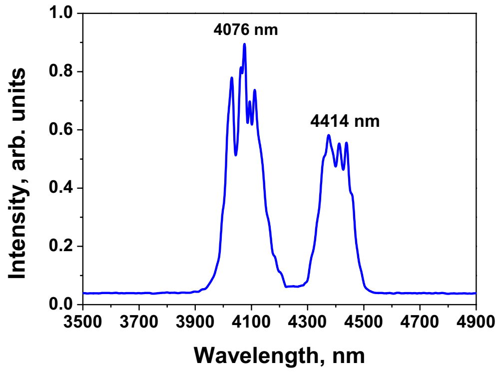

Fig. 9 The output spectrum of ZGP-OPO

a wing-pumping scheme. Under incident LD power of 25.6 W, the maximum CW output power of 10.5 W was obtained with a slope efficiency of 53.2%. Up to 41.0% diode-to-Ho conversion efficiency was realized. Under Q-switching operation, the maximum average output power of 9.8 W and maximum pulse energy of 3.7 mJ were obtained for PRF of 20 kHz and 3 kHz, respectively. Finally, we demonstrated an efficient mid-infrared laser based on diode-Ho-ZGP system. An average output power of 4.8 W was obtained at a PRF of 3 kHz. The optical conversion efficiency from LD to middle infrared was up to 18.8%.

Acknowledgements This work is supported by National Natural Science Foundation of China (51572053, 61378029 and 61775053), Science Foundation for Outstanding Youths of Heilongjiang Province (JC2016016), Science Foundation for Youths of Heilongjiang Province (QC2017078), and Fundamental Research funds for the Provincial Universities (Grant no. WL17B14).

References

1. G.J. Koch, J.Y. Beyon, B.W. Barnes, M. Petros, J. Yu, F. Amzajerdian, M.J. Kavaya, U.N. Singh, Opt. Eng. **46**, 116201 (2007)
2. T. Bach, T.R.W. Herrmann, C. Cellarius, A.J. Gross, World J. Urol. **25**, 263 (2007)
3. M. Schellhorn, G. Spindler, M. Eichhorn, Opt. Express **26**, 1402–1410 (2018)
4. K.S. Lai, P.B. Phua, R.F. Wu, Y.L. Lim, E. Lau, S.W. Toh, B.T. Toh, A. Chng, Opt. Lett. **25**, 1591 (2000)
5. T. Ehrenreich, R. Leveille, I. Majid, K. Tankala, G. Rines, P. Moulton, Proc. SPIE **7580**, 758016 (2010)
6. X.D. Mu, H. Meissner, H.C. Lee, Proc. SPIE **7686**, 76860T (2010)
7. Y. Shen, B. Yao, X. Duan, G. Zhu, W. Wang, Y. Ju, Y. Wang, Opt. Lett. **37**, 3558 (2012)
8. C.D. Nabors, J. Ochoa, T.Y. Fan, A. Sanchez, H.K. Choi, G.W. Turner, IEEE J. Quantum Electron. **31**, 1603 (1995)
9. K. Scholle, P. Fuhrberg, *Proceedings of CLEO, paper CTuAA1* (2008)
10. S. Lamrini, P. Koopmann, M. Schafer, K. Scholle, P. Fuhrberg, Appl. Phys. B **106**, 315 (2012)
11. S. Lamrini, P. Koopmann, M. Schäfer, K. Scholle, P. Fuhrberg, Opt. Lett. **37**, 515 (2012)
12. S. Lamrini, P. Koopmann, K. Scholle, P. Fuhrberg, Opt. Lett. **38**, 1948 (2013)
13. V. Jambunathan, X. Mateos, M.C. Pujol, J.J. Carvajal, M. Aguiló, F. Díaz, U. Griebner, V. Petrov, Appl. Phys. Express **4**, 072601 (2011)
14. G.A. Newburgh, M. Dubinskii, Proc. SPIE **8039**, 803905 (2011)
15. G.A. Newburgh, A. Word-Daniels, A. Michael, L.D. Merkle, A. Ikesue, M. Dubinskii, Opt. Express **19**, 3604 (2011)
16. A. Berrou, T. Ibach, M. Eichhorn, Appl. Phys. B **120**, 105 (2015)
17. E. Ji, Q. Liu, M. Nie, X. Cao, X. Fu, M. Gong, Opt. Lett. **41**, 1237 (2016)
18. E. Ji, Q. Liu, Y. Shen, M. Nie, X. Fu, IEEE Photonics Technol. Lett. **29**, 1695 (2017)
19. Q. Dong, G. Zhao, D. Cao, B. Yao, X. Yang, Z. Yu, J. Phys. D Appl. Phys. **42**, 045114 (2009)
20. B. Yao, X. Duan, L. Zheng, Y. Ju, Y. Wang, G. Zhao, Q. Dong, Opt. Express **16**, 14668 (2008)
21. T. Zhao, F. Wang, D.Y. Shen, Appl. Opt. **54**, 1594 (2015)
22. X. Duan, B. Yao, X. Yang, L. Li, T. Wang, Y. Ju, Y. Wang, G. Zhao, Q. Dong, Opt. Express **17**, 4427 (2009)
23. X.M. Duan, B.Q. Yao, X.T. Yang, T.H. Wang, Y.L. Ju, Y.Z. Wang, Appl. Phys. B **96**, 379 (2009)
24. Z. Cui, X.M. Duan, B.Q. Yao, J. Li, X.L. Li, T.Y. Dai, C.Y. Li, Y.B. Pan, Laser Phys. Lett. **12**, 105002 (2015)
25. T. Yu, X. Ye, Z. Yang, X. Chen, W. Xia, J. Zhang, W. Zhang, J. Chen, J. Si, W. Chen: Proc. SPIE **10173**, 101731M (2017)
26. X.M. Duan, W.M. Lin, Z. Cui, B.Q. Yao, H. Li, T.Y. Dai, Appl. Phys. B **122**, 88 (2016)